

Development of the Cathode Materials for Intermediate-Temperature SOFCs Based on Proton-Conducting Electrolytes



D. A. Medvedev and E. Yu. Pikalova

1 Introduction

The world is facing global climate change, a situation which calls for an effective low-carbon policy and efficient energy technologies. Energy technologies will also be crucial to achieving and maintaining a secure world energy supply. It is already evident that the use of standard technologies to produce electricity based on fossil fuels cannot satisfy the ever-growing demand for energy. The future for world energetic systems lies in the implementation of efficient and environmentally friendly technologies to produce electricity. From this perspective, hydrogen energy and fuel cells represent key technologies in attaining the renewable energy and emission reduction goals set worldwide [1].

Among the various kinds of fuel cells, solid oxide fuel cells (SOFCs) are advantageous because they are highly efficient at energy conversion and possess excellent fuel flexibility [2]. Principally, SOFCs can be divided into two main groups: the SOFC(O^{2-})s based on oxygen-conducting electrolytes (doped ZrO_2 , CeO_2 , Bi_2O_3 , and $LaGaO_3$) and the SOFC(H^+)s based on proton-conducting electrolytes (doped $BaCe(Zr)O_3$, $LaNbO_4$, $Ba_2In_2O_5$). High-temperature proton-conducting oxide materials laying in a base of SOFC(H^+)s are of great fundamental interest because of the phenomenon of proton conductivity which appears along with oxygen-ionic conductivity in a humidified atmosphere. The practical interest connected with the use of such Co-ionic electrolyte materials in intermediate-temperature solid oxide fuel cells (IT-SOFCs) stems from the increased efficiency due to higher open circuit voltage and, correspondingly, the power output characteristics in comparison with SOFCs based on unipolar oxygen-ion conducting

D. A. Medvedev (✉) · E. Y. Pikalova

Institute of High Temperature Electrochemistry, UB RAS, Yekaterinburg, Russia

Ural Federal University, Yekaterinburg, Russia

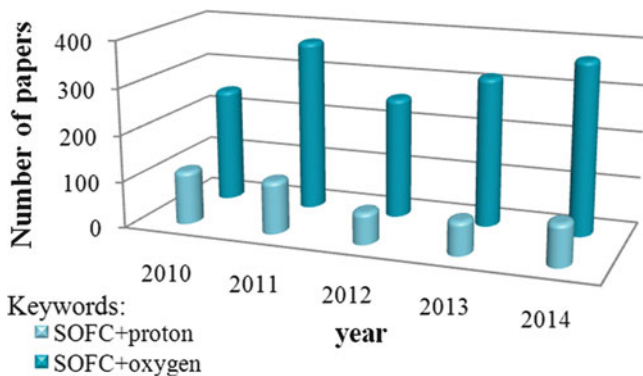


Fig. 1 Publication dynamics on the different search keywords in the SOFC field during the last 5 years (presented according to Scopus database)

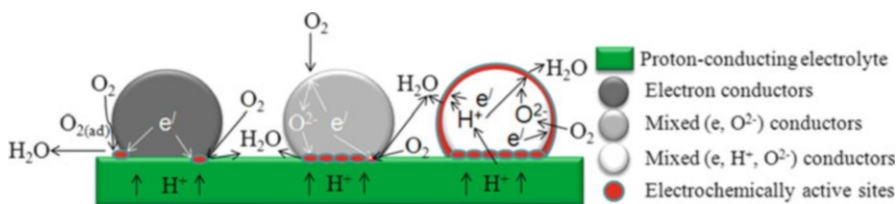


Fig. 2 Possible paths for the electrochemical reactions in cathode systems possessing different transport properties in contact with a proton-conducting electrolyte. The examples of electron conductors are Pt, and $\text{LaNi}_{0.6}\text{Fe}_{0.4}\text{O}_{3-\delta}$ [3], mixed (e^-, O^{2-}) conductor is $\text{GdBaCo}_2\text{O}_5 + \delta$ [3], and mixed $(e^-, \text{O}^{2-}, \text{H}^+)$ conductor is $\text{NdBa}_{0.5}\text{Sr}_{0.5}\text{Co}_{1.5}\text{Fe}_{0.5}\text{O}_5 + \delta$ [7]

electrolytes. Although SOFCs with protonic conductors are characterized by having the highest total efficiency (can exceed 80%) on account of thermodynamic and kinetic factors [3], they have been only moderately investigated compared to the SOFC(O^{2-})s (Fig. 1). Insofar as we know, there exists no commercial production of SOFC(H^+)s, one of the main reasons being the ongoing search for cathode materials that have all the necessary qualities for successful applications in contact with the optimal proton-conducting materials. To date there is much activity to enhance the SOFC's electrochemical characteristics by the development of new cathode materials which possess excellent electrocatalytic activity.

The first studies concerning SOFC(H^+) based on $\text{BaCe}(\text{Zr})\text{O}_3$ reported the use of a platinum cathode [3]. However, Pt is not preferred for practical applications due to its high cost. Moreover, the Pt electrodes were found to show significant polarization losses caused by the limited number of reaction sites at the cathode/electrolyte interface (Fig. 2). From this viewpoint, cathode materials with mixed oxygen-ionic and electronic conductivity widely used in SOFC(O^{2-})s so far as their application permits to significantly broaden the zone of electrochemical reaction (Fig. 2) [4] can be also applied in SOFC(H^+)s with Co-ionic conductors. However the development of an electrode material with proton conductivity would still be preferable since such

cathodes allow the simultaneous transport of ionic (proton, oxygen-ion) and electronic defects under typical fuel cell operating conditions, thus offering the potential to extend the active sites for oxygen and proton reactions and, correspondingly, decrease the polarization losses. Additionally, the electrodes must be thermodynamically stable under working conditions: $400\text{--}900\text{ }^\circ\text{C}$, $10^{-5} \leq p\text{O}_2/\text{atm} \leq 0.21$, in the presence of H_2O and CO_2 . Thermal affinity between electrolyte and cathode materials should be considered in order to attain both long-term stability and cycling.

Currently, there are many complex oxides that have been reported as having appropriate air electrode materials for SOFC(H^+). Regardless of the fact that very high short-term power densities ($\sim 0.4\text{ W cm}^{-2}$ at $600\text{ }^\circ\text{C}$, $\sim 1.0\text{ W cm}^{-2}$ at $700\text{ }^\circ\text{C}$) have been obtained recently for such an SOFC(H^+) [5–7], the issues associated with thermal affinity and chemical compatibility between electrolyte and cathode materials have not been precisely investigated. In this work the structural, electrical, and thermal properties of simple and layered cobaltites ($\text{GdBaCo}_2\text{O}_{5+\delta}$, $\text{NdBaCo}_2\text{O}_{5+\delta}$, $\text{Ba}_{0.5}\text{Sr}_{0.5}\text{CoO}_{3-\delta}$, $\text{Y}_{0.8}\text{Ca}_{0.2}\text{BaCo}_4\text{O}_{7+\delta}$), cobaltite-ferrites ($\text{NdBa}_{0.5}\text{Sr}_{0.5}\text{Co}_{1.5}\text{Fe}_{0.5}\text{O}_{5+\delta}$, $\text{GdBaCoFeO}_{5+\delta}$, $\text{Ba}_{0.5}\text{Sr}_{0.5}\text{Co}_{0.8}\text{Fe}_{0.2}\text{O}_{3-\delta}$, $\text{Ba}_{0.5}\text{Sr}_{0.5}\text{Co}_{0.2}\text{Fe}_{0.8}\text{O}_{3-\delta}$, $\text{La}_{0.6}\text{Sr}_{0.4}\text{Co}_{0.2}\text{Fe}_{0.8}\text{O}_3$), nickelite ($\text{La}_2\text{NiO}_{4+\delta}$), and nickelate ($\text{LaNi}_{0.6}\text{Fe}_{0.4}\text{O}_{3-\delta}$) were investigated in terms of their perspective applications in intermediate-temperature SOFCs in contact with the $\text{BaCe}_{0.8}\text{Y}_{0.2}\text{O}_{3-\delta}$ and $\text{BaZr}_{0.8}\text{Y}_{0.2}\text{O}_{3-\delta}$ proton-conducting electrolytes with special attention given to their chemical compatibility.

2 Experimental Details

In the present study the cathode materials, except for $\text{LaNi}_{0.6}\text{Fe}_{0.4}\text{O}_{3-\delta}$ (LNF), were successfully synthesized according to the solid-state reaction method using oxides and carbonates of corresponding metals with a purity of not less than 99% as precursors. The citrate-nitrate combustion method was used to produce a single-phase LNF product. The designation of these materials and temperatures of the final synthesis T_{synt} and sintering T_{sint} are presented in Table 1. After calcination and ball milling, the powders were dry-pressed into disks or bar-shaped samples at a pressure of about 150 MPa and sintered at individually adjusted temperatures T_{sint} , which exceeded those of the final synthesis by 50–150 $^\circ\text{C}$. The densities of the sintered specimens, determined from their geometrical size and weight, varied in the range of 85–95% of the theoretical value, calculated from the XRD data.

The electrolyte powders $\text{BaCe}_{0.8}\text{Y}_{0.2}\text{O}_{3-\delta}$ and $\text{BaZr}_{0.8}\text{Y}_{0.2}\text{O}_{3-\delta}$ were obtained by the citrate-nitrate combustion method. The precursors obtained were calcined at 1150 $^\circ\text{C}$ (5 h) and finally sintered at 1450 $^\circ\text{C}$ (5 h).

The synthesized powders' characteristics were determined by X-ray diffraction analysis (XRD, D/MAX-2200 Rigaku) using $\text{CuK}\alpha 1$ radiation. The identification of the materials' phase composition and crystal structure was performed by employing MDI Jade 6 software. The results of XRD analysis revealed the formation of single-phase structures for all the samples investigated, indicating the formation

Table 1 Chemical composition of the cathode materials and their temperatures of synthesis (T_{synt}) and sintering (T_{sint}) and soaking time (τ)

Composition	Designation	$T_{\text{synt}} (^{\circ}\text{C})/\tau$ (h)	$T_{\text{sint}} (^{\circ}\text{C})/\tau$ (h)	Space group
$\text{Ba}_{0.5}\text{Sr}_{0.5}\text{CoO}_{3-\delta}$	BSC	1050/5	1100/5	P63/mmc
$\text{GdBaCo}_2\text{O}_5 + \delta$	GBC	1050/5	1150/5	Pmmm
$\text{NdBaCo}_2\text{O}_5 + \delta$	NBC	1050/5	1150/5	P4/mmm
$\text{Y}_{0.8}\text{Ca}_{0.2}\text{BaCo}_4\text{O}_{7+\delta}$	YCBC	1050/5	1150/5	Cmc21
$\text{Ba}_{0.5}\text{Sr}_{0.5}\text{Co}_{0.2}\text{Fe}_{0.8}\text{O}_{3-\delta}$	BSCF28	1150/5	1200/5	Pm3m
$\text{Ba}_{0.5}\text{Sr}_{0.5}\text{Co}_{0.8}\text{Fe}_{0.2}\text{O}_{3-\delta}$	BSCF82	1100/5	1150/5	Pm3m
$\text{La}_{0.6}\text{Sr}_{0.4}\text{Co}_{0.2}\text{Fe}_{0.8}\text{O}_{3-\delta}$	LSCF	1150/5	1200/5	R3C
$\text{GdBaCoFeO}_5 + \delta$	GBCF	1100/5	1150/5	P4/mmm
$\text{NdBa}_{0.5}\text{Sr}_{0.5}\text{Co}_{1.5}\text{Fe}_{0.5}\text{O}_{5+\delta}$	NBSCF	1100/5	1200/5	Pm3m
$\text{Ba}_{0.5}\text{Sr}_{0.5}\text{FeO}_{3-\delta}$	BSF	1200/10	1350/5	Pm3m
$\text{La}_{0.75}\text{Sr}_{0.2}\text{MnO}_{3-\delta}$	LSM	1200/10	1350/5	R3C
$\text{La}_2\text{NiO}_4 + \delta$	LN	1300/10	1450/5	Fmmm
$\text{LaNi}_{0.6}\text{Fe}_{0.4}\text{O}_{3-\delta}$	LNF	1300/10	1450/5	R3C

of solid-state solutions. Corresponding data on crystal symmetry are listed in Table 1.

In order to estimate the chemical compatibility, the powdered cathode materials were thoroughly mixed with electrolyte powders in the weight ratio 1:1, calcined at 1100 °C for 10 h, and then analyzed by XRD. The calcination temperature was selected based on the literature data which show that the cathode functional layers usually form on the electrolyte surface at 1100 °C.

The thermal expansion of the materials was carried out using a Tesatronic TT-80 dilatometer between room temperature and 900 °C with a heating/cooling rate of 3 °C min⁻¹ in an air atmosphere. The average thermal expansion coefficients (TECs) were found from the fitting of the linear region of the dilatometric curves.

The conductivity of the samples was investigated at 500–900 °C in air by a standard four-probe dc method utilizing the microprocessor system ZIRCONIA-318.

3 Results and Discussion

3.1 Chemical Compatibility

After calcination at 1100 °C for 10 h, the XRD analysis was used to determine the characteristics of the powders' mixtures of the electrode and electrolyte materials and to estimate the degree of chemical interaction between them. It was found that the BCY electrolyte possesses a low chemical stability in contact with most of the cathode compositions. Although the structures of the main phases in

Table 2 Summary results of chemical and thermal compatibilities and electrical properties of the investigated cathode materials. The gray color of cells indicates the appropriate properties. The chemical expansion is marked by * symbol

Designation	Impurity phase(s)		$\alpha \cdot 10^6$ (K ⁻¹)	σ (S cm ⁻¹)	
	BCY	BZY		600 (°C)	700 (°C)
BSC	CeO ₂ , SrO	No interaction	15.6	420	385
GBC	CeO ₂ , BaCoO _x , BaO	No interaction	21.3	430	330
NBC	BaCoO _x , BaCoNd ₂ O ₇	YBa ₂ Fe ₃ O ₈	23.1*	925	795
YCBC	CeO ₂ , YBaCo ₂ O ₅ , YBa ₂ Co ₃ O ₉	No interaction	9.6	90	105
BSCF28	No interaction	No interaction	26.0*	15	11
BSCF82	CeO ₂ , SrO, BaO	YBa ₂ Fe ₃ O ₈ , BaO, Fe ₂ O ₃	16.6*	580	530
LSCF	La ₂ CoO ₄	YBa ₂ Fe ₃ O ₈	19.9*	205	190
GBCF	CeO ₂ , BaCoO _x , Fe ₃ O ₄ , BaGd ₂ FeO ₇	No interaction	17.2	40	35
NBSCF	BaCoO _x , Sr(Fe,Co)O ₃	No interaction	26.9*	360	305
BSF	No interaction	No interaction	34.1*	11	7
LSM	CeO ₂ , YMn ₂ O ₅	Mn ₃ O ₄	10.7	140	115
LN	No interaction	No interaction	13.1	70	60
LNF	No interaction	No interaction	14.5	515	500

electrolyte/cathode mixtures remained the same as before treatment, different impurities and phases of interaction appeared (Table 2):

- CeO₂ for BSC, GBC, YCBC, BSCF82, GBCF, and LSM.
- SrO for BSC and BSCF82.
- Barium cobaltites for GBC, NBC, GBCF, and NBSCF and strontium cobaltite for LSCF.
- BaO and SrO for GBC and BSCF82, respectively.
- BaCoNd₂O₇ for NBC, La₂CoO₄ for LSCF, Fe₃O₄ for GBCF, Sr(Fe,Co)O₃ for NBSCF, YMn₂O₅ for LSM, and BaGd₂FeO₇ for GBCF.

The Y_{0.8}Ca_{0.2}BaCo₄O_{7 + δ} layered perovskite phase completely decomposes in the mixture with cerate after a treatment for 10 h at 1100 °C: YBaCo₂O₅, YBa₂Co₃O₉, and CeO₂ phases are fixed along with the main BaCeO₃ structure.

No significant interaction was observed in the calcined mixtures of BCY with BSCF28, BSF, LN, and LNF.

The obtained data confirm previously presented results for Co-containing electrode materials [8], showing an active Co-diffusion from cobaltites into BaCeO₃-based electrolytes and, as a consequence, the formation of BaO, BaCoO₂, and BaCoO₃

impurities. The decrease in Co-ions concentration results in some suppression of the impurity phase formation in the sequence $\text{Ba}_{0.5}\text{Sr}_{0.5}\text{CoO}_{3-\delta}$ – $\text{Ba}_{0.5}\text{Sr}_{0.5}\text{Co}_{0.8}\text{Fe}_{0.2}\text{O}_{3-\delta}$ – $\text{Ba}_{0.5}\text{Sr}_{0.5}\text{Co}_{0.2}\text{Fe}_{0.8}\text{O}_{3-\delta}$ – $\text{Ba}_{0.5}\text{Sr}_{0.5}\text{FeO}_{3-\delta}$. For example, no impurity phases were detected in the mixture of BSF and BCY. The chemical activity of the cerate electrolyte with double cobaltites seems to be higher than that with simple cobaltite since formation of secondary phases was detected for all the calcined mixtures, containing $\text{LnBaCo}_2\text{O}_{5+\delta}$ -based oxides.

BaZrO_3 -based electrolyte being the material with higher tolerance factor (t) shows better chemical stability than the barium cerate in agreement with the concept of Goldschmidt [9]. As in the case of barium cerate, an interaction of the barium zirconate with cobaltites (NBC and LSCF) was detected and also with manganite (LSM) but to a lesser degree (trace amount of $\text{YBa}_2\text{Fe}_3\text{O}_8$ and Mn_3O_4 were detected, respectively). A high degree of chemical interaction was observed for the BSCF82 in contact with BZY material with the appearance of some secondary phases.

3.2 Thermal Compatibility

Investigation of the thermal properties of the cathode materials is critical in terms of evaluating their adhesion and the quality of the interface contact and, correspondingly, maintaining the mechanical stability of the electrolyte/electrode assembly during the formation and operation of the SOFCs.

However, studies have revealed that materials which possess excellent catalytic activity and transport properties such as simple and layered cobaltites show the TEC values to be more than $20 \cdot 10^{-6} \text{ K}^{-1}$ which is 1.5–3 times higher than those measured for BCY and BZY which are $8\text{--}12 \cdot 10^{-6} \text{ K}^{-1}$ (Table 2). It makes their application in contact with the BCY and BZY electrolytes questionable.

For the cobaltites, the strategy of partial substitution of Co-ions by other transition metals ($M = \text{Fe}, \text{Ni}, \text{Cu}$) or of the cation on A-site of Co-based perovskite by a cation with a lower ionic radius is usually adopted in order to decrease TEC values [3, 4, 11]. The comparison of thermal data for $\text{GdBaCo}_2\text{O}_{5+\delta}$ ($21.3 \cdot 10^{-6} \text{ K}^{-1}$) and $\text{GdBaCoFeO}_{5+\delta}$ ($17.2 \cdot 10^{-6} \text{ K}^{-1}$) confirms the proposed strategy. However, for many cobaltite-ferrites (LSCF, BSF, BSCF28, BSCF82, NBSCF), the thermal expansion behavior deviates from linearity resulting in the intense expansion of ceramics in the high-temperature range in comparison with that in the low-temperature range. This can probably be attributed to the unwanted chemical expansion caused by the presence of elements in different oxidation and spin states [10].

3.3 Electrical Compatibility

Conductivity of the cathode materials is one of the most important properties necessary for optimum performance with properties such as low polarization, serial, and in-plane resistances [4, 11]. As long as the porosity of the electrode layers after formation and co-sintering with the electrolyte surface averages 25–40%, the conductivity of the compact electrode samples should be no less than 100 S/cm. The conductivity of the cathode materials decreases when increasing the temperature in the interval of 500–900 °C which indicates its metallic type. Most of the developed materials possess an acceptable conductivity at 600 and 700 °C, except BSCF28, BSF, and GBCF (Table 2). The conductivity for LN and YCBC samples registered intermediate values. Therefore their application is preferable in combination with conductors that have high electronic conductivity.

4 Conclusion

In the present work, different cathode materials were successfully prepared and their structural, thermal, and electrical properties and chemical compatibility with the electrolytes were thoroughly investigated to find the appropriate compositions for their eventual application in SOFC(H⁺) with BaCeO₃ and BaZrO₃ proton-conducting electrolytes.

Analysis of the experimental data has shown that, if taking into account all the abovementioned properties, LaNi_{0.6}Fe_{0.4}O_{3- δ} and La₂NiO_{4 + δ} electrode materials are the most suitable as the cathodes in contact with BaCe_{0.8}Y_{0.2}O_{3 - δ} and BaZr_{0.8}Y_{0.2}O_{3 - δ} proton-conducting electrolytes for intermediate-temperature SOFCs.

The layered Y_{0.8}Ca_{0.2}BaCo₄O_{7 + δ} cobaltite has the closest TEC value with those for cerate and zirconate ceramics; however, it completely decomposes after a treatment of Y_{0.8}Ca_{0.2}BaCo₄O_{7 + δ} /BaCe_{0.8}Y_{0.2}O_{3 - δ} mixture and can be recommended only for usage in contact with BaZr_{0.8}Y_{0.2}O_{3 - δ} electrolyte.

Acknowledgments This work is supported by the Russian Foundation for Basic Research (grant № 13-03-00065); Program of UD RAS (project № 15-20-3-15), by Act 211 Government of the Russian Federation (contract № 02.A03.21.0006); and the Council of the President of the Russian Federation (grant № ЦП-1885.2015.1).

References

1. Fuel Cell and Hydrogen technologies in Europe-Financial and technology outlook on the European sector ambition 2014–2020, New Energy World. <http://www.new-ig.eu/hydrogen-fuel-cells>

2. Mahato, N., Banerjee, A., Gupta, A., Omar, S., Balan, K.: Progress in material selection for solid oxide fuel cell technology: A review. *Prog. Mater. Sci.* **72**, 141–337 (2015)
3. Medvedev, D., Murashkina, A., Pikalova, E., Demin, A., Podias, A., Tsiakaras, P.: BaCeO₃: Materials development, properties and application. *Prog. Mater. Sci.* **60**, 72–129 (2014)
4. Tsiapis, E.V., Kharton, V.V.: Electrode materials and reaction mechanisms in solid oxide fuel cells: A brief review. I. Performance-determining factors. *J. Solid State Electrochem.* **12**, 1039–1060 (2008)
5. Min, S.H., Song, R.-H., Lee, J.G., Park, M.-G., Ryu, K.H., Jeon, Y.-K., Shul, Y.-G.: Fabrication of anode-supported tubular Ba(Zr_{0.1}Ce_{0.7}Y_{0.2})O_{3-δ} cell for intermediate temperature solid oxide fuel cells. *Ceram. Int.* **40**, 1513–1518 (2014)
6. Nien, S.H., Hsu, C.S., Chang, C.L., Hwang, B.H.: Preparation of BaZr_{0.1}Ce_{0.7}Y_{0.2}O_{3-δ} based solid fuel cells with anode functional layers by tape casting. *Fuel Cells.* **11**, 178–183 (2011)
7. Kim, J., Sengodan, S., Kwon, G., Ding, D., Shin, J., Liu, M., Kim, G.: Triple-conducting layered perovskites as cathode materials for proton-conducting solid oxide fuel cells. *ChemSusChem.* **7**, 2811–2815 (2014)
8. Lin, Y., Ran, R., Zhang, C., Cai, R., Shao, Z.: Performance of PrBaCo₂O_{5+δ} as a proton-conducting solid-oxide fuel cell cathode. *J. Phys. Chem. A.* **114**, 3764–3772 (2010)
9. Sammells, A.F., Cook, R.L., White, J.H., Osborne, J.J., MacDuff, R.C.: Rational selection of advanced solid electrolytes for intermediate temperature fuel cells. *Solid State Ionics.* **52**, 111–123 (1992)
10. Yaremchenko, A.A., Mikhalev, S.M., Kravchenko, E.S., Frade, J.R.: Thermochemical expansion of mixed-conducting (Ba,Sr)Co_{0.8}Fe_{0.2}O_{3-δ} ceramics. *J. Eur. Ceram. Soc.* **34**, 703–715 (2014)
11. Tucker, M.C., Cheng, L., DeJonghe, L.C.: Selection of cathode contact materials for solid oxide fuel cells. *J. Power Sources.* **196**, 8313–8322 (2011)